however, there have been only a few reports about ABR in intracochlear schwannoma. Gersdorff et al. [6] reported an increase in the absolute latency of the first peak in ABR. In their case, PTA showed a mean threshold of 85 dB for frequencies between 250 and 2,000 Hz. The curve was ascendant for the higher frequency, and the threshold at 8 kHz was 30 dB; however, schwannoma was pointed out in the basal turn of the cochlea and in the fundus of IAC. Therefore, the cochlear partitions occupied by schwannoma in the cochlea were different from those related to hearing loss in the audiogram. Thus, hearing loss in their case may be the retrocochlear type rather than cochlear. On the other hand, in our case, ABR was normal at the beginning of follow-up. Considering the relationship between hearing loss in the audiogram and the occupation of schwannnoma in the cochlea, hearing loss was first interpreted as a cochlear disorder. During follow-up before profound deafness, the hearing threshold increased gradually and equally at all frequencies. Considering that the schwannoma had invaded the fundus of the IAC, the progress of hearing loss may be caused mainly by retrocochlear disorders due to invasion. When PTA showed profound hearing loss in the right ear, TEOAE, DPOAE and ABR were absent. This is probably because both cochlear and retrocochlear lesions caused too severe deafness for any recordings to be possible. Thus, when schwannoma localizes in the cochlea, the ABR test probably does not show retrocochlear disorders. Observation of the retrocochlear type in the ABR test is the finding to indicate the possibility of the invasion into IAC.

Intracochlear schwannoma may be difficult to diagnose even with gadolinium-enhanced MRI [7]. However, in our case, a gadolinium-enhancing lesion was detected in the cochlea, and we suspected intracochlear schwannoma. While Donnelly et al. [8] indicated the usefulness of the CISS sequence in defining intracochlear lesions, the CISS image in our case was also of great benefit to the evaluation of intracochlear schwannoma. Thus, the development of the imaging technology help the diagnosis of intracochlear schwannoma. As our case, intracochlear schwannoma will be diagnosed at the early stage with mild hearing loss in the future, if appropriate examination and evaluation are performed. In order not to overlook it, it is necessary to pay attention to abnormal lesions within the cochlea or vestibule, and a suspicious lesion should be confirmed by a repeat scan.

References

1. Vernick DM, Graham MD, McClatchey KD (1984) Intralabyrinthine schwannoma. Laryngoscope 94:1241–1243
2. Huang TS (1986) Primary intralabyrinthine schwannoma. Ann Otol Rhinol Laryngol 95:190–192
3. Sataloff RT, Roberts BR, Feldman M (1988) Intralabyrinthine schwannoma. Am J Otol 9:323–326
4. Kronenberg J, Horowitz Z, Hildesheimer M (1999) Intracochlear schwannoma and cochlear implantation. Ann Otol Rhinol Laryngol 108:659–660
5. Ohtani I, Suzuki C, Aikawa T (1990) Temporal bone pathology in intracochlear schwannoma with profound hearing loss. Auris Nasus Larynx 17:17–22
6. Gersdorff MC, Decat M, Duprez T, Deggouj N (1996) Intracochlear schwannoma. Eur Arch Otorhinolaryngol 253:374–376
7. Green JD Jr, McKenzie JD (1999) Diagnosis and management of intralabyrinthine schwannomas. Laryngoscope 109:1626–1631
8. Donnelly MJ, Daly CA, Briggs RJ (1994) MR imaging features of an intracochlear acoustic schwannoma. J Laryngol Otol 108:1111–1114

Neuroscience Letters 438 (2008) 260–262

Contents lists available at ScienceDirect

Neuroscience Letters

journal homepage: www.elsevier.com/locate/neulet

Assessment of ability to discriminate frequency of bone-conducted ultrasound by mismatch fields

Akinori Yamashita [a,*], Tadashi Nishimura [a], Seiji Nakagawa [b], Takefumi Sakaguchi [a], Hiroshi Hosoi [a]

[a] Department of Otolaryngology, Nara Medical University, 840 Shijo-cho, Kashihara, Nara 634-8522, Japan
[b] Institute for Human Science and Biomedical Engineering, National Institute of Advance Industrial Science and Technology (AIST), 1-8-31 Midorigaoka, Ikeda, Osaka 563-8577, Japan

ARTICLE INFO

Article history:
Received 25 June 2007
Received in revised form 21 December 2007
Accepted 30 March 2008

Keywords:
Ultrasound
Magnetoencephalography
Bone conduction
Mismatch fields
Frequency modulation

ABSTRACT

According to previous studies, ultrasound can be perceived through bone conduction and ultrasound amplitude modulated by different speech sounds can be discriminated by some profoundly deaf subjects as well as the normal-hearing. These findings suggest the usefulness of development of a bone-conducted ultrasonic hearing aid (BCUHA) for profoundly deaf subjects. In this study, with a view to developing a frequency modulation system in a BCUHA, the capability to discriminate the frequency of sinusoidal bone-conducted ultrasound (BCU) was evaluated by measuring mismatch fields (MMF). We compared MMFs between BCU (standard stimuli were 30 kHz, and deviant stimuli were 27 and 33 kHz) and air-conducted audible sound (ACAS; standard stimuli were 1 kHz, and deviant stimuli were 900 and 1100 Hz). MMFs were observed in all subjects for ACAS, however, not observed in a few subjects for BCU. Further, the mean peak amplitudes of MMF for BCU were significantly less than those for ACAS. These findings indicate that the discrimination capability of frequency of sinusoidal BCU is inferior to that of ACAS. It was also demonstrated that normal hearing could to some extent discriminate differences in frequency in sinusoidal BCU. The results indicate a possibility of transmission system for language information making use of frequency discrimination.

Generally speaking, human listeners perceive sound signals through air conduction from 20 to 20,000 Hz. Sound with frequency over 20 kHz is termed "ultrasound". Until half a century ago, it was thought that ultrasound could not be perceived. However, Gavreau reported in 1948 that ultrasound was audible when delivered by bone conduction [5]. Several researchers subsequently reported interesting perceptual characteristics of bone-conducted ultrasound (BCU), which differ markedly from those of audible sound. For instance, the subjective pitch of BCU is independent of its frequency [2,3] and it is perceived as if it were from air-conducted stimuli of 8–16 kHz [2,3,10]. In addition, BCU can mask perception of air-conducted audible sound (ACAS) of 10–14 kHz and this masking of ACAS is independent of ultrasonic frequency. The dynamic range of BCU is narrower than that of ACAS [9]. Interestingly, some profoundly deaf patients can hear BCU. Lenhardt et al. reported that BCU hearing supported frequency discrimination and speech detection in some deaf patients as well as normal-hearing subjects by [7]. Furthermore, Hosoi et al. found using magnetoencephalography that BCU stimuli activate the auditory cortex, and that ultrasound amplitude modulated by different speech sounds can be discriminated in the auditory cortex in some profoundly deaf subjects [6]. These findings suggest the possibility of development of a bone-conducted ultrasonic hearing aid (BCUHA), which could be used by elderly hearing-impaired and profoundly deaf subjects [8].

For development of such a hearing aid, it is necessary to determine the most effective method of transmission of language information. Corso founded that BCU perception is characterized by poor frequency discrimination, although auditory perception in ACAS is characterized by excellent frequency discrimination [1]. This has been concluded from the finding that subjective pitch elicited by BCU stimulation is independent of its frequency and similar to that for the highest ACAS. Lenhardt, using a psychoacoustical method, reported that just noticeable pitch differences in the ultrasonic range were on the order of 10% of the stimulus frequency, although that in the auditory range were between 0.4 and 1.0% [7]. These studies have found that ability to discriminate the frequency of BCU is inferior to that of ACAS. However, no study has

* Corresponding author. Tel.: +81 744 29 8887; fax: +81 744 24 6844.
E-mail address: akinori@naramed-u.ac.jp (A. Yamashita).

0304-3940/$ – see front matter © 2008 Elsevier Ireland Ltd. All rights reserved.
doi:10.1016/j.neulet.2008.03.086

evaluated ability to discriminate the frequency of sinusoidal BCU objectively. In this study, to assess a possibility of development of a frequency modulation system in a BCUHA, we measured discrimination capability of the frequency of sinusoidal BCU by magnetoencephalography.

Twelve right-handed volunteers (aged 20–30 years, 4 females and 8 males) with normal hearing and no history of neurological diseases took part in the study. They gave written informed consent after being informed of the nature and purpose of this study.

To evaluate capability to discriminate BCU, comparison was made with capability to discriminate ACAS since previous studies more frequently used ACAS than BCU. We measured mismatch fields (MMFs) for BCU and ACAS, in cases in which the frequency deviated 10% from standard frequency. BCU and ACAS were presented in separate sequences. Each sequence consisted of a standard stimulus (probability 90%) and two types of deviant stimuli (probability 5% each), with all stimuli delivered in random order to the subject. More than 100 responses evoked by deviant stimuli were averaged. After averaging of MMFs, one of the deviant stimuli was continually and successively delivered more than 100 times as a comparison stimulus. The other deviant stimulus was then delivered in the same fashion. In a sequence of BCU, we used 30 kHz BCU as a standard stimulus and 27 and 33 kHz BCU as deviants and comparison stimuli. On the other hand, in ACAS sequences, we used 1000 Hz ACAS as a standard stimulus and 900 and 1100 Hz ACAS as deviant and comparison stimuli. The intensities of BCU and ACAS were set at 15 and 60 dB SL, respectively. The duration was set at 50 ms, including 5 ms rise/fall times, and the interstimulus interval was varied randomely between 0.9 and 1.1 ms. During the experiment, the subject was watching a self-chosen movie without sound and was instructed to pay no attention to the auditory stimuli.

Recording of the brain activation evoked by BCU and ACAS was performed in a magnetically shielded room using a 122-channel whole-head neuromagnetometer (Neuromag-122; Neuromag Ltd., Helsinki, Finland). All the sounds were generated by a function generator (WF1946; NF Electronic Instruments Co., Yokohama, Japan). The ultrasound signal was increased through a high-speed power amplifier (HSA4011; NF Electronic Instruments Co, Yokohama, Japan). Sound intensity was controlled by a programmable attenuator in the dB scale (PA4; Tucker–Davis Technologies, Gainesville, FL). Ultrasound was delivered with a custom-made ceramic vibrator for MEG fixed on the left mastoid. The ACAS was emitted using an earphone (E-A-R TONE3A, Cabot Safety Co., Indianapolis, IN), and was delivered to the left ear through a plastic tube. MEG signals were measured, having been digitized at 400 Hz, and were band-pass-filtered through 0.03–100 Hz. Any responses including greater than 3000 fT/cm changes were rejected from further analysis. Averaged data were band-pass-filtered through 0.1–30 Hz off-line. The duration of analysis was 0.7 s, beginning 0.2 s prior to stimulus onset. The average during the 0.2 s prestimulus period served as the baseline. The neuromagnetometer used in this experiment has two pick-up coils in each position, which measure tangential derivatives, $\delta Bz/\delta x$ and $\delta Bz/\delta y$, of field component Bz. We determined:

$$B' = \sqrt{\left(\frac{\delta Bz}{\delta x}\right)^2 + \left(\frac{\delta Bz}{\delta y}\right)^2},$$

as the amplitude of the response. For determination of the MMF amplitude of each subject, we employed the maximum $B'z$ placed over the right temporal area.

The MMF was delineated by subtracting the comparison-stimulus responses from the deviant-stimulus response separately for each sequence and deviant type. We defined MMF as follows: peak latency ranged from 100 to 300 ms, peak amplitude was greater than 10 fT/cm, and the estimated equivalent current dipole was over the right temporal area and turned downward. We employed a channel where the largest MMF peak amplitude was observed with all stimuli. With this channel, each MMF peak amplitude and latency were measured. Amplitudes were normalized to the respective values obtained at the largest MMF peak amplitude in each subject. Differences in peak amplitude and peak latency between BCU and ACAS responses were tested for significance by two-ways ANOVA.

Clear N1m responses were observed in all subjects for all type of stimuli. N1m responses for all stimuli showed the maximum amplitude during 80 to 116 ms. Fig. 1 shows the response waveforms in a subject for 33 kHz BCU and 1100 Hz ACAS. In this subject, clear N1m and MMF responses were observed for all stimuli.

All subjects replied to detect the pitch change with change in frequency of ACAS and BCU. Although MMFs were observed in all subjects for ACAS, not observed in 3 subjects for 27-kHz and 1 subject for 33-kHz BCUs. The delineated MMF was elicited at

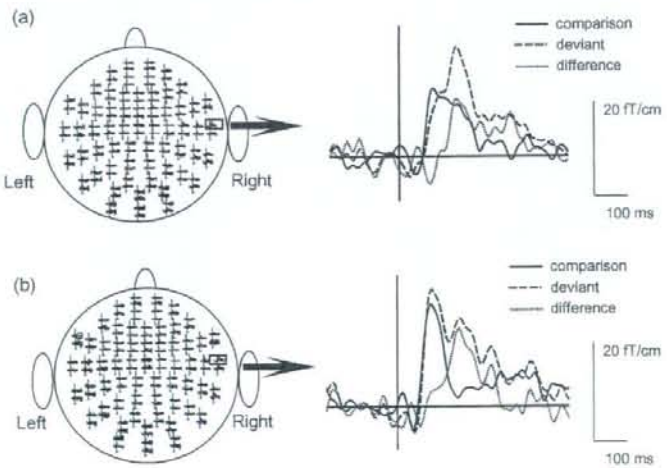

Fig. 1. Wave forms in a subject evoked by (a) 33-kHz BCU and (b) 1100-Hz ACAS. The sensor locations are shown in the left part, and the waveforms in the largest responses measured in the MEG channels in the right temporal region are enlarged in the right part.

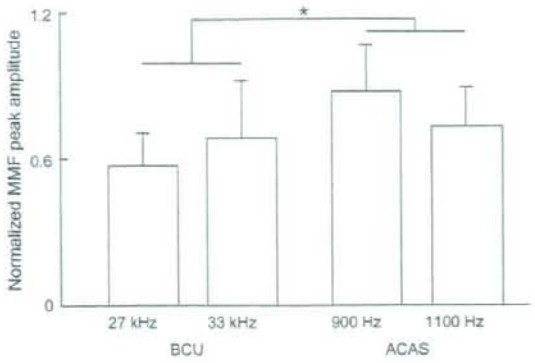

Fig. 2. Mean MMF peak amplitudes for BCU and ACAS. Vertical bars indicate standard deviations.

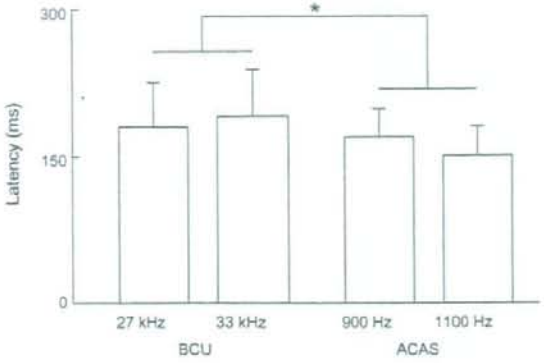

Fig. 3. Mean MMF peak latencies for BCU and ACAS. Vertical bars indicate standard deviations.

latencies of 180–200 ms for all frequencies. Fig. 2 shows normalized MMF peak amplitude. The mean peak amplitudes for BCU (27 and 33 kHz) were significantly less than those for ACAS (900 and 1100 Hz) ($p < 0.05$). Fig. 3 shows the mean peak latencies of MMF. The mean peak latencies for BCU were significantly later than those for ACAS ($p < 0.05$).

Although MMFs were observed in all subjects for ACAS, however, in only 9 and 11 subjects for 27- and 33-kHz BCUs, respectively. Even in case MMF were observed for BCU, MMF peak amplitude in BCU reached about three-fourths of that for ACAS. The peak amplitudes for BCU were significantly less than those for ACAS. Thus, capability to discriminate the frequency of BCU was inferior to that of ACAS, in agreement with previous reports.

Although most subjects detected pitch change with change in frequency of BCU, the amount of pitch change exhibited marked variation among our subjects. Previous studies reported similar findings; the subjective pitch elicited by ultrasonic stimulation was independent of its frequency, and it is perceived as if it were from air-conducted stimuli of 8–16 kHz. These characteristics of ultrasonic perception indicate that the pitch of BCU fluctuates and that pitch change is unstable. That is, the amount of pitch change exhibits large individual variation with a given change in stimulus frequency. In the range of ultrasonic frequency, increase in frequency does not always lead to subjective increase in pitch. These characteristic changes in pitch in the ultrasonic range may have been responsible for the variation in MMF we observed.

If BCU is to be used as a means of communication, language information must be modulated to within the ultrasonic range using amplitude modulation, frequency modulation, or so. For development of ultrasonic hearing aids, it will be necessary to determine which type of modulation is more effective. Fujimoto et al. reported good capability of frequency discrimination of BCU by amplitude modulation. The difference limens for frequency for pure tones modulated onto ultrasonic carriers was as small as that for air-conducted pure tones at 0.25–4 kHz [4]. On the other hand, no previous study has investigated ability to discriminate BCU using frequency modulation. The present study evaluated capability to discriminate frequency in sinusoidal BCU objectively using MEG. Our results objectively demonstrated that capability to discriminate the frequency of BCU was inferior to that of ACAS. However, it was also demonstrated that normal hearing could to some extent discriminate differences in frequency in sinusoidal BCU. In addition, it may be possible to improve frequency discrimination capability by training or improvement of sound processing. Therefore, further investigation is needed to determine the most appropriate transmission system for language information using ultrasound.

The present findings provide important clues to the development of the BCUHA. However, the characteristics of BCU hearing and the mechanisms of perception of BCU are still unclear. Further study is needed for development of the BCUHA in elderly hearing-impaired and profoundly deaf subjects.

References

[1] J.F. Corso, Bone-conduction thresholds for sonic and ultrasonic frequencies, J. Acoust. Soc. Am. 35 (1963) 1738–1743.
[2] B.H. Deatherage, L.A. Jeffress, H.C. Blodgett, A note on the audibility of intense ultrasonic sound, J. Acoust. Soc. Am. 26 (1954) 582.
[3] H.G. Dieroff, H. Ertel, Some thoughts on the perception of ultrasound by name, Arch. Otorhinolaryng 209 (1975) 277–290.
[4] K. Fujimoto, S. Nakagawa, M. Tonoike, Nonlinear explanation for bone-conducted ultrasonic hearing, Hear. Res. 204 (2005) 210–215.
[5] V. Gavreau, Audibilite de sons frequence elevee, C. R. 226 (1948) 2053–2054.
[6] H. Hosoi, S. Imaizumi, T. Sakaguchi, M. Tonoike, K. Murata, Activation of the auditory cortex by ultrasound, Lancet 351 (1998) 496–497.
[7] M.L. Lenhardt, R. Skellett, P. Wang, A.M. Clarke, Human ultrasonic speech perception, Science 253 (1991) 82–85.
[8] S. Nakagawa, Y. Okamoto, Y. Fujisaka, Development of a Bone-conducted Ultrasonic Hearing Aid for the Profoundly Sensorineural Deaf, Trans. Jpn. Soc. Med. Biol. Eng. 44 (1) (2006) 184–189.
[9] T. Nishimura, S. Nakagawa, T. Sakaguchi, H. Hosoi, Ultrasonic masker clarifies ultrasonic perception in man, Hear. Res. 175 (2003) 171–177.
[10] R. Pumphrey, Upper limit of frequency for human hearing, Nature 166 (1950) 571.

Ultrasonics 48 (2008) 607–612

Contents lists available at ScienceDirect

Ultrasonics

journal homepage: www.elsevier.com/locate/ultras

Numerical and experimental study on the wave attenuation in bone – FDTD simulation of ultrasound propagation in cancellous bone

Yoshiki Nagatani [a,*], Katsunori Mizuno [b,1], Takashi Saeki [b,1], Mami Matsukawa [b,1], Takefumi Sakaguchi [a,2], Hiroshi Hosoi [a,2]

[a] Department of Otorhinolaryngology, Nara Medical University, 840 Shijo-cho, Kashihara, Nara 634-8522, Japan
[b] Graduate School of Engineering, Doshisha University, 1-3 Miyakodani, Tatara, Kyotanabe, Kyoto 610-0321, Japan

ARTICLE INFO

Article history:
Received 20 August 2007
Received in revised form 23 April 2008
Accepted 23 April 2008
Available online 13 May 2008

Keywords:
Cancellous bone
Fast wave
X-ray CT
Three-dimensional elastic FDTD method

ABSTRACT

In cancellous bone, longitudinal waves often separate into fast and slow waves depending on the alignment of bone trabeculae in the propagation path. This interesting phenomenon becomes an effective tool for the diagnosis of osteoporosis because wave propagation behavior depends on the bone structure. Since the fast wave mainly propagates in trabeculae, this wave is considered to reflect the structure of trabeculae. For a new diagnosis method using the information of this fast wave, therefore, it is necessary to understand the generation mechanism and propagation behavior precisely. In this study, the generation process of fast wave was examined by numerical simulations using elastic finite-difference time-domain (FDTD) method and experimental measurements. As simulation models, three-dimensional X-ray computer tomography (CT) data of actual bone samples were used. Simulation and experimental results showed that the attenuation of fast wave was always higher in the early state of propagation, and they gradually decreased as the wave propagated in bone. This phenomenon is supposed to come from the complicated propagating paths of fast waves in cancellous bone.

1. Introduction

More reliable and less onerous diagnosis of osteoporosis is now expected in this aging society. Ultrasonic diagnosis system is considered as a strong tool, because ultrasonic wave reflects the elasticity. The current *in vivo* ultrasonic diagnosis technique called speed of sound/broadband ultrasound attenuation (SOS/BUA) method [1] is a simple indicator to describe bone properties. The SOS/BUA method gives the averaged ultrasonic wave speed and attenuation in a whole area including soft tissue, cortical bone, and cancellous bone, which seems difficult to show the complicated bone structure and the amount of mineral materials of each part. Therefore, a new index that can reflect detailed structure of bone is now required: e.g. Padilla et al. and Jenson et al. proposed a new indicator using backscattered wave from bone sample [2–4].

In order to improve the accuracy of ultrasonic diagnosis systems, our group has proposed a new evaluation idea, making use of the separation of longitudinal waves that pass through the cancellous bone [5–7]. We have reported the separation of longitudinal waves into fast and slow waves, especially depending on the alignment of bone trabeculae in cancellous bone. This interesting phenomenon is considered to become a strong tool for the diagnosis of osteoporosis because the wave propagation behavior apparently depends on the bone structure. However, the details of wave propagation in cancellous bone are not fully understood, because of the structural complexity and inhomogeneity of the bone.

In order to understand the wave propagation phenomena in the cancellous bone, there were some theoretical approaches. By Biot's theory [8,9] or stratified model [10], with the help of several parameters to describe the bone structure, we can predict the generation of fast and slow waves in cancellous bone. However, the selection of parameters such as porosity, bulk and shear moduli of solid part, fluid viscosity and permeability in Biot's theory seems to be very difficult.

One recent approach to understand the wave propagation is the direct analysis of wave equation. If the 3-D numerical simulation of wave propagation is successfully performed, it shall give us the visual image of complicated wave propagation in the bone. Luo et al. have reported the simulation results of wave propagation in cancellous bone using microCT model [11]. They investigated the wave speed and the attenuation values, however, they did not discuss the wave separation into fast and slow waves. Hosokawa has first reported the wave separation by a numerical solution of Biot's theory with finite-difference method [12]. Using a 3-D synchrotron

* Corresponding author. Tel.: +81 744 22 3051; fax: +81 744 24 6844.
E-mail addresses: naramed-u@nagatani.ne.jp (Y. Nagatani), mmatsuka@mail.doshisha.ac.jp (M. Matsukawa).
[1] Tel.: +81 774 65 6292; fax: +81 774 65 6801.
[2] Tel.: +81 744 22 3051; fax: +81 744 24 6844.

0041-624X/$ - see front matter © 2008 Elsevier B.V. All rights reserved.
doi:10.1016/j.ultras.2008.04.011

micro tomography of actual trabeculae, Bossy et al. [13] and Padilla et al. [14,15] have reported the generation of fast and slow waves using finite-difference time-domain (FDTD) simulation. Haiat et al. have investigated the influence of trabeculae bone microstructure and material properties on QUS parameters using numerical simulations [16]. Our group has also tried to confirm the applicability of elastic FDTD method for the simulation of two-waves propagation in cancellous bone using three-dimensional X-ray CT images [17,18]. In these studies, we have reported the accordance between the FDTD simulation and experimental results. We also confirmed that the simulated peak amplitudes ratio of fast and slow waves showed accordance with the experimental results. Since the positions and conditions of sound source or receivers are easy to be changed in simulation, the FDTD analysis of wave propagation using actual CT data is useful not only for understanding the behavior of sound wave but also for an optimal design of a new diagnostic system.

In this two-wave propagation phenomenon, the fast wave mainly propagates in trabeculae and reflects its structure [17–19]. This means that the fast wave provides information on the trabeculae structure. In this study, therefore, by simulating the fast wave propagation in the cancellous bone, we especially aimed at clarifying the mechanism of fast wave generation focusing on the attenuation. We also checked the adequacy of the simulated results by comparing them to experimental results using actual bone samples.

2. Elastic FDTD method

The followings are the governing equations of three-dimensional elastic FDTD method for the isotropic medium related to x direction

$$\frac{\partial \sigma_{xx}}{\partial t} = (\lambda + 2\mu)\frac{\partial v_x}{\partial x} + \lambda\frac{\partial v_y}{\partial y} + \lambda\frac{\partial v_z}{\partial z}, \quad (1)$$

$$\frac{\partial \sigma_{xy}}{\partial t} = \mu\left(\frac{\partial v_x}{\partial y} + \frac{\partial v_y}{\partial x}\right), \quad (2)$$

$$\frac{\partial v_x}{\partial t} = \frac{1}{\rho}\left(\frac{\partial \sigma_{xx}}{\partial x} + \frac{\partial \sigma_{xy}}{\partial y} + \frac{\partial \sigma_{zx}}{\partial z}\right), \quad (3)$$

where σ_{ij} is normal and shear stresses, v_i is particle velocity, λ and μ are Lame's coefficients, ρ is density of the medium. In this simulation, the elastic anisotropy in the solid part was not considered. Using the same equations for y and z directions, the stress and particle velocity were calculated alternately both in the spatial and time-domains, which was called 'leapfrog method' [20]. Here, the absorption in both media was not introduced, however, it was confirmed by our group that the amplitude ratio of fast wave and slow wave was in good agreement with the experimental results [5–6].

3. Simulation model and measurement system

3.1. FDTD simulation model

For FDTD simulation, three parallelepipedic bovine cancellous bone samples A, B and C were used. The size of three samples used were 15 × 15 × 9–12 mm. Fig. 1a and b are the examples of X-ray micro focus CT images (SMX-100CT, SHIMADZU, Kyoto, Japan). The samples were obtained from the femoral head of 36 months old bovine. Spatial resolution of the CT images was 46 μm. Here, the resolution of the CT model of human cancellous bone used by Haiat et al. was 30 μm [21]. The mean thickness of bovine cancellous bones is larger than human bones. The reported mean thickness of human trabeculae is from 50–150 μm [22], whereas that ob bovine bone is from 150–200 μm. Therefore, the spatial resolution of our simulation model seems reasonable. The value at each point in

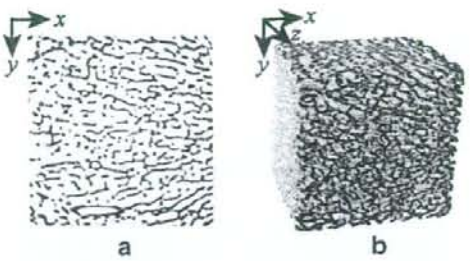

Fig. 1. An X-ray CT image of bovine sample used in numerical simulation. (a) Two-dimensional X-ray CT image of sample B. (b) Three-dimensional X-ray CT image of sample B.

the CT images was binarized in order to separate the ambiguous border between solid parts (trabeculae) and liquid parts with a specific threshold. The threshold was decided as the median value of the grayscale tones of the image.

The total simulation field was 17 × 17 × 13 mm with cube lattice of 46 μm. This is the maximum size for our computer memory (4GB). Time step was 4 ns. As the initial particle velocity at the surface of the plane source shown in Fig. 2. The initial waveform comes from the experimentally observed waveform of a single sinusoidal sound wave at 1 MHz that passed through the water. In order to avoid the strong instabilities of the simulation, the waveform was treated with low-pass filter whose cut-off frequency was 10 MHz. The filtered waveform is shown in Fig. 3. In this model, the bone sample was fully immersed in water.

As the speed of longitudinal wave in the solid part of the cancellous bone, the experimentally observed values of bovine cortical bone in the MHz range were used [23–26]. The speed of the shear wave was an estimated value, assuming the Poisson's ratio of 0.35. The parameters used in this simulation are shown in Table 1. The FDTD simulation software was originally programmed by our group [27].

In the first simulation, the wave propagated from the top to bottom surfaces. The propagating direction is parallel to the bone

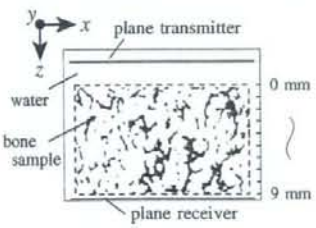

Fig. 2. Simulation model. A plane transmitter faces towards the sample immersed in water.

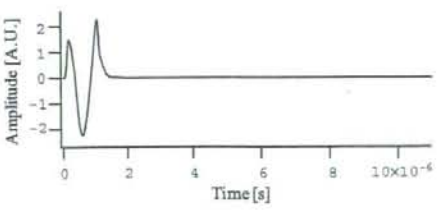

Fig. 3. Initial particle velocity.

Table 1
Parameters used in the FDTD simulation

Material		Water	Bone trabecula
Density [10^3kg/m^3]		1.0	2.0
Velocity [m/s]	Longitudinal	1500	3500
	Shear	-	2400

axes. In order to evaluate the attenuation of propagating waves in bone, the sample was virtually ground gradually from the bottom surfaces. The samples were shorten gradually from 9 to 1 mm thickness with an interval of 1 mm. Using the sample of smaller thickness, the simulation was performed again. By comparing the amplitudes of the first peak of calculated waveforms obtained at each thickness, the spatial distribution of the attenuation in the sample was obtained. The attenuation value a is calculated by the following equation:

$$a = \frac{20\log(V_n/V_{n+1})}{\Delta x}, \tag{4}$$

where V_n is the first peak amplitude of fast wave when the thickness of specimen is n mm, Δx is thickness difference between the measurements.

In the second simulation, the wave propagated from the bottom to top surfaces. We also obtained the spatial distribution of attenuation by filing away the sample from the top surface.

3.2. Measurement system for experiments

The attenuation measurements were also performed experimentally. The size of bone samples was 20 × 20 × 15 mm. The samples were obtained from the same part in the femoral head of 36 months old bovine. During measurements, the bone sample was immersed in degassed water in an acoustical tube at room temperature. The surface area of the plane PVDF transmitter and receiver (self-made, using PVDF films) were 20 × 20 mm. This comparatively large transducer brings good signal to noise ratio of the observed waves. The distance between two transducers was 60 mm.

A single sinusoidal wave at 1 MHz, with amplitude of 5 V_{p-p} (peak to peak voltage) from a function generator (WF1945, NF Corporation, Kanagawa, Japan) was amplified 20 dB by a power amplifier (4055, NF Corporation, Kanagawa, Japan), and applied to the transmitter. The waves that passed through the sample from top to bottom surfaces were investigated by a digital oscilloscope (TDS 524A, Tektronix Inc., Oregon, United States) with 40 dB preamplifier (5307, NF Corporation, Kanagawa, Japan). The propagating direction was parallel to the bone axes.

Similar to the FDTD studies, the thickness of actual specimens was filed away from the bottom surface. The measurements were done using samples changing thickness from 15 to 6 mm.

4. Results and discussion

4.1. Numerical results

Some examples of simulated waveforms are shown in Fig. 4. Fig. 4a shows the result when the wave passed through reference water alone. The small fluctuation in the wave tail comes from the instability of simulation, mainly due to the high-frequency component of the initial waveform. The fluctuation, however, was never observed in the area of fast wave. Fig. 4b shows the result when the sample was 9 mm thick and c shows the result of the sample 5 mm thick. In both waveforms of Fig. 4b and c, fast and slow waves can be seen. The amplitudes of the fast waves were always much smaller than those of the slow waves, which has also been reported in the experimental studies [5–7]. From the peak amplitudes of fast waves, the distribution of attenuation [dB/mm] can be evaluated; e.g. using peak amplitudes of 9 mm thick and 8 mm thick, we obtained the distribution of attenuation values between the positions of 8 to 9 mm from the surface.

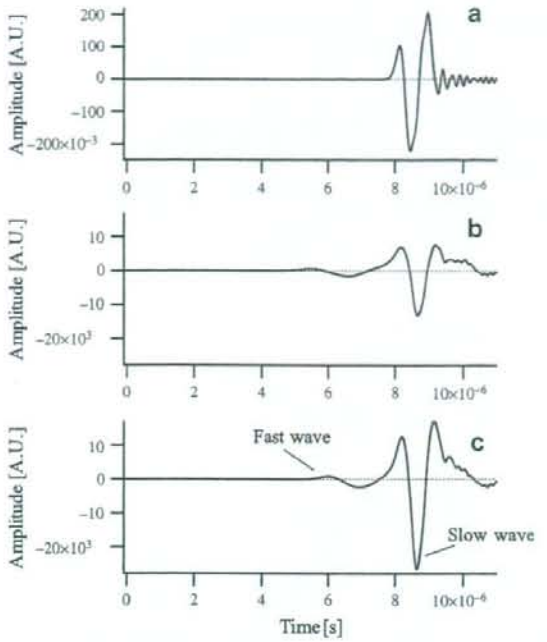

Fig. 4. Numerically simulated waveforms. (a) Without sample. (b) With sample of 9 mm thick. (c) With sample of 5 mm thick.

The distribution of BV/TV (bone volume/total volume) and fast wave attenuation of three specimens are shown in Figs. 5 and 6. The BV/TV was obtained from each 1 mm slice of three-dimensional model of bone constructed by CT data. The area of solid part was numerically examined in each slice. Fig. 6a shows the results when the wave propagated from top surface and b shows the results from the bottom surface. Here, the values of horizontal position axis mean the observed position from the top surface. These data show that the attenuation of fast wave is always higher in the early state of propagation. As the wave propagates in the bone, the attenuation gradually decreased and became almost constant.

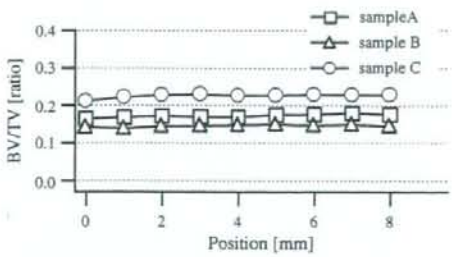

Fig. 5. Distributions of bone volume fraction of tree samples used in simulation.

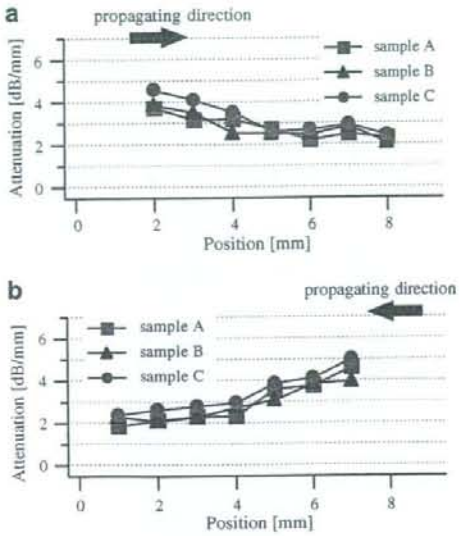

Fig. 6. Distributions of numerically simulated fast wave attenuation. (a) Attenuation when the wave propagated from top surface. (b) Attenuation when the wave propagated from bottom surface.

4.2. Experimental results

Some examples of the experimentally observed waveforms are shown in Fig. 7. Fig. 7b is the result when the specimen was 9 mm thick and c was 5 mm thick. Fast and slow waves can be seen in both waveforms.

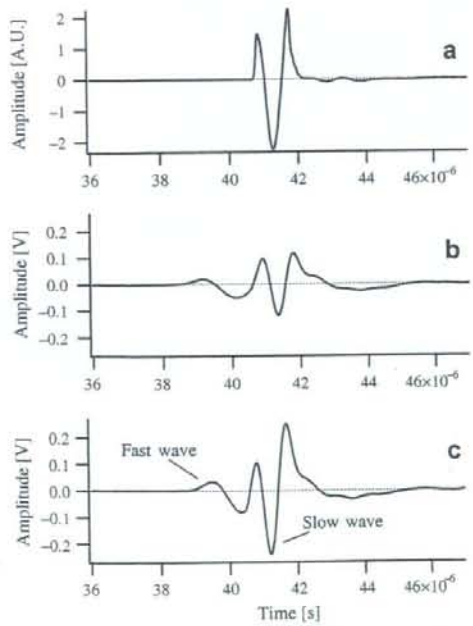

Fig. 7. Experimentally observed waveforms. (a) Without sample. (b) With sample of 9 mm thick. (c) With sample of 5 mm thick.

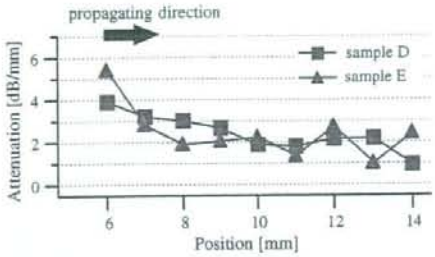

Fig. 8. Distributions of experimentally observed fast wave attenuation.

From the peak amplitudes of fast waves that passed through the sample with different thickness, the attenuation value at each position was obtained. Fig. 8 shows the attenuation of fast wave when the wave was transmitted from top surface. Similar to the simulation results, fast wave attenuation decreased due to the wave propagation. For direct comparison of simulation and experiments, we have measured the identical specimen D used for the simulation. The data is shown in Fig. 9. Due to the memory limitation, the simulation was done using the center part of the experi-

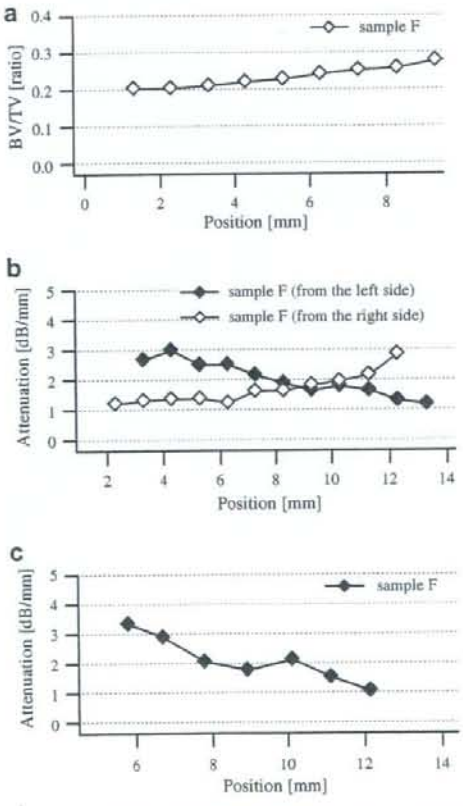

Fig. 9. Comparison of fast wave attenuation between the simulation and experiments. The sample used in simulation and experiment is identical. (a) Distributions of bone volume fraction of the sample. (b) Numerically simulated results of fast wave attenuation. (c) Experimentally observed results of fast wave attenuation.

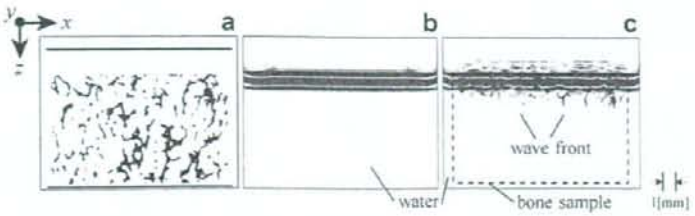

Fig. 10. Bone model and screenshots of the distribution of sound pressure at the central x–y plane of the three-dimensional simulation field. (a) Bone model. The black structure indicates solid part (trabecula). (b) Screenshot without sample at 2.5 μs. Clear wavefront can be seen. (c) Screenshot with sample at 2.5 μs. Fast and slow waves can be seen.

mentally measured specimen. Here, we can again find the reasonable accordance in the behavior of attenuation.

4.3. Discussions

In this study, the precise attenuation of slow waves could not be obtained because the amplitudes were often affected by the superposition of fast wave. As can be seen in Fig. 7, the amplitudes of fast wave sometimes reach around 10% of the amplitudes of slow wave, which induces the effect on the attenuation of slow waves.

In both simulated and experimental results, attenuation values of fast wave were the highest at the beginning. The attenuation of fast wave, then, decreased monotonously and finally showed almost steady value. The monotonous decreases were similar in all samples with comparatively constant BV/TV, telling poor dependence on the structure fluctuation. This becomes clearer in Fig. 9 of the direct comparison between the simulation and experiments. The attenuation behavior was similar in both simulation and experiments, showing the higher attenuation at the beginning. The comparatively small simulated attenuation at the beginning of the propagation from the bottom seems to come from the larger BV/TV values of this area. Considering the large amount of trabeculae in this area, the attenuation of fast wave is possibly small.

One reason for this interesting attenuation phenomenon is considered to come from the complicated propagation path of propagating waves. The fast wave mainly propagates in the trabeculae of cancellous bone [17–19]. The alignment of the trabeculae is not always parallel to the direction of propagation. This implies that there is some dispersion in the propagating path of fast wave due to the random alignment of trabeculae. Fig. 10a, b and c show the screenshots of the distribution of sound pressure (in liquid portion) or root-mean-square value of normal stresses (in solid portion) at the central x–y plane of the three-dimensional simulation field. The bone model is shown in Fig. 10a. The black structure indicates solid part (trabeculae). For comparison, Fig. 10b shows the distribution of sound pressure of wave in water. We can see clear wave front in Fig. 10b. Fig. 10c is the result of the wave that passed through the bone model. The complicated wave front can also be seen. We can also see fast wave propagation in bone model, which corresponds with the trabeculae structure. Due to the various paths, the wavefront position of fast wave would not be uniform in this state. This irregularity of wave front then seems to cause the apparent higher attenuation of fast wave. In addition, as can be seen in Figs. 4 and 7, the fast wave peaks were always separated from the slow wave in this simulation and measured data. This possibly indicates little effects of slow waves on the first peak of fast wave in this state. However, one should note that the mutual effects of fast and slow waves should be considered in the exact initial state of wave propagation.

These results tell us that the fast wave requires certain propagation distance to form in-phase wave front and steady attenuation. This also means that the fast wave attenuation is difficult to be used as an indicator of the structural properties of cancellous bone for the characterization of thin cancellous bone samples.

5. Conclusion

Using the 3-D X-ray CT model of a bovine cancellous bone, the attenuation of fast waves was discussed by numerical simulation and experiments. The attenuation of fast wave was higher in the early state of propagation and gradually decreased as the propagation proceeds. This tells us the fast wave requires certain propagation distance for steady propagation. It seems then that the fast wave attenuation is not suitable as a parameter for precise evaluation of thin cancellous bone.

Acknowledgments

Authors would appreciate the measurement of X-ray micro focus CT to Shimadzu Corporation. Authors would also appreciate the processing of bone samples to Ms. Najac Marion at Ecole Superieure de Physique et de Chimie Industrielles in Paris.

This study was partly supported by a bilateral joint project between JSPS and CNRS, in addition to the Academic Research Frontier project of Doshisha University and Ministry of Education, Culture, Sports, Science and Technology in Japan. Some parts of this study were also supported by the project, "Open Competition for the Development of Innovative Technology" of Ministry of Education, Culture, Sports, Science and Technology. This work was also supported by Grants-in-Aid for Research on Indoor Environmental Medicine of Nara Medical University.

References

[1] C.F. Njeh, D. Hans, T. Fuerst, Quantitative Ultrasound: Assessment of Osteoporosis and Bone Status, first ed., Taylor & Francis, 1999.
[2] F. Padilla, F. Peyrin, P. Laugier, Prediction of backscatter coefficient in trabecular bones using a numerical model of 3D microstructure, J. Acoust. Soc. Am. 113 (2) (2003) 1122–1129.
[3] F. Jenson, F. Padilla, P. Laugier, Prediction of frequency-dependent ultrasonic backscatter in cancellous bone using statistical weak scattering model, Ultrasound. Med. Biol. 29 (3) (2003) 455–464.
[4] F. Jenson, F. Padilla, V. Bousson, C. Bergot, J.-D. Laredo, P. Laugier, In vitro ultrasonic characterization of human cancellous femoral bone using transmission and backscatter measurements: Relationships to bone mineral density, J. Acoust. Soc. Am. 119 (1) (2006) 654–663.
[5] A. Hosokawa, T. Otani, Ultrasonic wave propagation in bovine cancellous bone, J. Acoust. Soc. Am. 101 (1997) 558–562.
[6] A. Hosokawa, T. Otani, T. Suzaki, Y. Kubo, S. Takai, Influences of trabecular structure on ultrasonic wave propagation in bovine cancellous bone, Jpn. J. Appl. Phys. 36 (5B) (1997) 3233–3237.
[7] T. Otani, Quantitative estimation of bone density and bone quality using acoustic parameters of cancellous bone for fast and slow waves, Jpn. J. Appl. Phys. 44 (6B) (2005) 4578.

[8] M.A. Biot, Generalized theory of acoustic wave propagation in porous dissipative media, J. Acoust. Soc. Am. 34 (1962) 1254–1264.
[9] K.A. Lee, H.S. Roh, S.W. Yoon, Acoustic wave propagation in bovine cancellous bone: application of the modified Biot-Attenborough model, J. Acoust Soc. Am. 114 (2003) 2284–2293.
[10] K.A. Wear, A stratified model to predict dispersion in trabecular bone, IEEE. Trans. Ultrason. Ferroelectr. Freq. Control 48 (4) (2001) 1079–1083.
[11] G. Luo, J.J. Kaufman, A. Chiabrera, B. Bianco, J.H. Kinney, D. Haupt, J.T. Ryaby, R.S. Siffert, Computational methods for ultrasonic bone assessment, Ultrasound. Med. Biol. 25 (5) (1999) 823–830.
[12] A. Hosokawa, Simulation of ultrasound propagation through bovine cancellous bone using elastic and Biot's finite-difference time-domain methods, J. Acoust. Soc. Am. 118 (2005) 1782–1789.
[13] E. Bossy, F. Padilla, F. Peyrin, P. Laugier, Three-dimensional simulation of ultrasound propagation through trabecular bone structures measured by synchrotron microtomography, Phys. Med. Biol. 50 (2005) 5545–5556.
[14] F. Padilla, E. Bossy, G. Haïat, F. Jenson, P. Laugier, Numerical simulation of ultrasound transmission in cancellous bone, in: Ultrasonics Symposium, 2005 IEEE, vol. 4, 2005, pp. 2022–2025.
[15] F. Padilla, E. Bossy, P. Laugier, Simulation of ultrasound propagation through three-dimensional trabecular bone structures: Comparison with experimental data, Jpn. J. Appl. Phys. 45 (8A) (2006) 6496–6500.
[16] G. Haïat, F. Padilla, F. Peyrin, P. Laugier, Variation of ultrasonic parameters with microstructure and material properties of trabecular bone: A 3D model simulation, J. Bone. Miner. Res. 22 (5) (2007) 665–674.
[17] Y. Nagatani, H. Imaizumi, T. Fukuda, M. Matsukawa, Y. Watanabe, T. Otani, Applicability of finite-difference time-domain method to simulation of wave propagation in cancellous bone, Jpn. J. Appl. Phys. 45 (9A) (2006) 7186–7190.
[18] Y. Nagatani, H. Imaizumi, T. Fukuda, M. Matsukawa, Yoshiaki Watanabe, Takahiko Otani, FDTD Simulation on the wave propagation in the cancellous Bone, 8e Congres Francaise d'Acoustique – Proceedings, 2006, 681–684..
[19] L. Cardoso, F. Teboul, L. Sedel, C. Oddou, A. Meunier, In vitro acoustic waves propagation in human and bovine cancellous bone, J. Bone. Miner. Res. 18 (2003) 1803–1812.
[20] K.S. Yee, Numerical solution of initial boundary value problems involving Maxwell's equations in isotropic media, IEEE. Trans. Antennas Propag. AP-14 (3) (1966) 302–307.
[21] G. Haïat, F. Padilla, R. Barkmann, C.C. Glüer, P. Laugier, Numerical simulation of the dependence of quantitative ultrasonic parameters on trabecular bone microarchitecture and elastic constants, Ultrasonics 44 (2006) e289–e294.
[22] S. Chaffai, V. Roberjot, F. Peyrin, G. Berger, P. Laugier, Frequency dependence of ultrasonic backscattering in cancellous bone: Autocorrelation model and experimental results, J. Acoust. Soc. Am. 108 (2000) 2403–2411.
[23] Y. Yamato, H. Kataoka, M. Matsukawa, K. Yamazaki, T. Otani, A. Nagano, Distribution of longitudinal wave velocities in bovine cortical bone in vitro, Jpn. J. Appl. Phys. 44 (6B) (2005) 4622–4624.
[24] Y. Yamato, M. Matsukawa, T. Otani, K. Yamazaki, A. Nagano, Distribution of longitudinal wave properties in bovine cortical bone in vitro, Ultrasonics 44 (2006) e233–e237.
[25] Y. Yamato, M. Matsukawa, K. Yamazaki, H. Mizukawa, T. Yanagitani, A. Nagano, Correlation between hydroxyapatite crystallite orientation and ultrasonic wave velocities in bovine cortical bone, Calcif. Tissue Int. 82 (2008) 162–169.
[26] M. Sasso, G. Haïat, Y. Yamato, S. Naili, M. Matsukawa, Frequency dependence of ultrasonic attenuation in bovine cortical bone: An in vitro study, Ultrasound. Med. Biol. 33 (2007) 1933–1942.
[27] Y. Tanikaga, T. Sakaguchi and Y. Watanabe, A study on analysis of intracranial acoustic wave propagation by finite difference time domain method, in: Proceedings of Forum Acusticum, Sevilla, 2002.

日本音響学会誌 64 巻 11 号 (2008), pp. 647-649

技術報告

親密度別単語了解度試験用音声データセット (FW03) 単音節音声のラウドネス校正*

長谷芳樹*1 橘 亮輔*2 阪口剛史*1 細井裕司*1

[要旨] 近年，日本語単語及び単音節の聴取実験に「親密度別単語了解度試験用音声データセット (FW03)」(NII 音声資源コンソーシアム，2006) が広く用いられている。しかし，FW03 の音声レベルは等価騒音レベルが等しくなるよう校正されているため，特に単音節音声の聴感レベルが試験語ごとに大きく異なるという問題があった。そこで我々は，単音節音声について聴取実験によるラウドネス校正を行い，その校正値を公開することとした。実験の結果，必要な補正量は最大で 12 dB を超えていた。FW03 の単音節音声を用いる際には，この校正値を適用することが望ましい。

キーワード FW03，単音節，ラウドネス，校正
FW03, Monosyllabic speech sounds, Loudness, Calibration

1. はじめに

近年，日本語単語及び単音節の聴取実験に「親密度別単語了解度試験用音声データセット (FW03) [1]」が広く用いられている。FW03 には，坂本らが提案した親密度別単語リスト 4,000 語 [2] と，日本語単音節 100 音節について，それぞれ男女 2 名ずつ，計 4 名の話者 (fhi, fto, mis, mya) の音声が収録されている。しかし，FW03 の音声レベルは等価騒音レベルが等しくなるよう校正されているため，特に単音節音声の聴感レベルが試験語ごとに大きく異なるという問題があった [3]。

坂本らは語音聴取閾値 (Speech Reception Threshold：SRT) による聴感レベル校正を行っている [3] が，一般に SRT を揃えても語音のラウドネスが一致するとは限らない。このため，ラウドネスの違いが何等かの手掛かりとなって，聴取実験等に悪影響を及ぼす可能性がある。

このため我々は，聴取実験により FW03 単音節音声のラウドネス校正を進めてきた [4]。今回，4 話者の校正値の策定が完了したため，報告する。

2. 実験方法

日本語を母語とする健聴 (純音聴力検査 4 分法 30 dBHL 以内) な男女 (23～30 歳) を被験者とした。被験者数は，話者 fhi と mis について 21 名，fto と mya について 19 名の，延べ 40 名であった。刺激は防音室内でオージオメータ (モリタ，SA-50A 及びリオン，AA-76) の気導受話器を通じて聴力の良い片耳に呈示した。呈示レベルは，FW03 に収録されている 1 kHz 校正音が 60 dBSPL となるように設定した。

基準音節を/a/，比較音節を/a/を除く 99 音節からランダムに選んだ 1 音節とし，これらを交互に繰り返し呈示して，ラウドネスが等しくなるまで比較音節の音圧を被験者に調整させた。基準音節の等価騒音レベルは常に 60 dB となるように固定した。音圧の調整は 1 dB 刻みとし，操作はすべて PC に接続されたマウスで行わせた。試行開始時の音圧は，予備実験で得られた話者及び音節ごとの値を中心とし，平均値 −9～−12 dB もしくは平均値 +9～+12 dB の範囲からランダムに設定した。オンセット間間隔は 500 ms とした。なお，各音節の平均時間長は約 300 ms であった。

比較音節が/a/以外の音節である 99 試行に加えて，比較音節が基準音節と同じ/a/である試行をランダムに 5 回挿入した。その 5 試行の結果の最大値と最小値の差が 6 dB 以上となっている被験者は解析対象から除外した。結果，有効標本数は，話者 fhi, fto, mis, mya につきそれぞれ 19 名であった。また，各音節の結果から，最大値と最小値を除外した。

3. 結果

結果の平均値と標準誤差を表–1 に示す。これは，それぞれの話者の/a/を 0 dB としたとき，各音節を記載のレベルで呈示した場合にラウドネスが等しく知覚さ

* Loudness calibration of monosyllabic speech sounds in FW03,
by Yoshiki Nagatani, Ryosuke Tachibana, Takefumi Sakaguchi and Hiroshi Hosoi.

*1 奈良県立医科大学医学部耳鼻咽喉・頭頸部外科学講座
*2 同志社大学大学院工学研究科知覚・認知機構研究室
(問合先：長谷芳樹 〒651-2194 神戸市西区学園東町 8-3 神戸市立工業高等専門学校)

(2008 年 5 月 9 日受付，2008 年 6 月 30 日採録決定)

表-1 FW03 単音節音声のラウドネス校正値 [dB]

音節	fhi		fto		mis		mya	
	平均	S.E.	平均	S.E.	平均	S.E.	平均	S.E.
あ	—	—	—	—	—	—	—	—
い	−8.0	0.6	−6.1	0.6	−6.8	0.7	−8.6	0.7
う	−7.2	0.9	−6.0	0.4	−10.5	0.6	−8.5	0.8
え	−4.0	0.6	−5.0	0.7	−5.2	0.4	−5.5	0.6
お	−5.2	0.6	−3.3	0.8	−5.3	0.5	−4.2	0.7
か	−0.3	0.4	−2.2	0.5	−0.9	0.4	0.2	0.6
き	−5.7	0.6	−8.1	0.7	−7.9	0.7	−6.2	0.4
く	−7.0	0.8	−5.8	0.8	−10.1	0.5	−7.9	0.7
け	−5.4	0.7	−5.7	0.4	−6.0	0.4	−5.6	0.6
こ	−1.1	0.5	−2.2	0.5	−2.4	0.6	−3.5	0.5
さ	−1.5	0.6	−0.6	0.5	−2.5	0.7	−2.3	0.5
し	−8.5	0.7	−8.7	0.8	−8.4	0.6	−9.6	0.5
す	−7.0	0.8	−8.1	0.6	−10.5	0.6	−9.6	0.5
せ	−8.0	0.7	−6.7	0.7	−7.6	0.5	−6.6	0.8
そ	−6.9	0.7	−3.2	0.7	−5.8	0.7	−3.5	0.4
た	−0.9	0.6	−0.6	0.6	−0.3	0.5	−1.4	0.5
ち	−7.5	0.8	−5.9	0.6	−7.3	0.7	−4.9	0.8
つ	−8.0	0.5	−7.2	0.6	−10.4	0.5	−9.2	0.4
て	−5.2	0.7	−5.3	0.5	−6.4	0.4	−5.8	0.4
と	−3.3	0.5	−1.2	0.5	−3.4	0.6	−3.5	0.6
な	−3.6	0.4	0.1	0.5	−4.2	0.7	−2.2	0.5
に	−5.9	0.7	−4.8	0.7	−6.2	0.6	−9.2	0.9
ぬ	−7.0	0.5	−5.2	0.5	−11.1	0.7	−9.3	0.6
ね	−7.9	0.4	−2.8	0.6	−6.2	0.5	−5.6	0.6
の	−5.9	0.5	−3.5	0.6	−4.5	0.5	−3.5	0.4
は	1.7	0.6	−0.5	0.6	−0.8	0.5	−2.1	0.5
ひ	−6.5	0.7	−6.2	0.6	−6.6	0.7	−7.6	0.6
ふ	−9.5	0.8	−6.0	0.6	−12.6	0.5	−7.1	0.5
へ	−6.4	0.5	−5.0	0.5	−6.4	0.6	−5.2	0.7
ほ	−5.1	0.6	−1.7	0.8	−4.1	0.4	−3.9	0.6
ま	−0.1	0.4	−2.8	0.5	−2.3	0.4	−1.5	0.3
み	−6.1	0.7	−5.5	0.8	−7.5	0.7	−7.8	0.8
む	−6.3	0.6	−5.6	0.7	−7.9	0.6	−10.5	0.7
め	−5.6	0.6	−5.0	0.6	−5.8	0.4	−6.4	0.5
も	−2.5	0.6	−1.2	0.5	−7.3	0.5	−4.1	0.6
や	−2.4	0.6	−1.4	0.6	−1.4	0.6	−4.1	0.4
ゆ	−6.3	0.7	−6.6	0.6	−9.8	0.6	−9.0	0.5
よ	−5.2	0.6	−3.2	0.9	−4.8	0.4	−2.6	0.6
ら	−0.8	0.6	1.9	0.4	0.3	0.5	−0.8	0.5
り	−7.6	0.8	−7.1	0.5	−9.2	0.5	−6.2	0.7
る	−7.3	0.7	−7.4	0.6	−9.3	0.7	−7.2	0.6
れ	−5.8	0.5	−3.8	0.7	−5.2	0.5	−5.8	0.6
ろ	−4.6	0.6	−1.5	0.5	−2.9	0.3	−3.8	0.6
わ	−0.5	0.5	0.5	0.6	0.8	0.5	−0.2	0.5
が	−0.6	0.5	0.5	0.5	−2.6	0.4	−0.8	0.5
ぎ	−7.3	0.6	−7.6	0.5	−9.0	0.7	−8.4	0.4
ぐ	−5.1	0.7	−5.8	0.8	−10.1	0.7	−9.6	0.4
げ	−5.5	0.5	−4.9	0.5	−5.5	0.7	−6.6	0.4
ご	−5.1	0.6	−2.5	0.7	−7.1	0.5	−3.8	0.5

音節	fhi		fto		mis		mya	
	平均	S.E.	平均	S.E.	平均	S.E.	平均	S.E.
ざ	−4.5	0.4	−0.9	0.4	−2.2	0.6	−1.6	0.5
じ	−6.8	0.4	−5.9	0.5	−9.4	0.6	−8.0	0.8
ず	−9.1	0.6	−7.8	0.5	−11.6	0.8	−8.1	0.5
ぜ	−7.5	0.5	−4.5	0.6	−5.4	0.6	−5.1	0.6
ぞ	−5.5	0.4	−2.2	0.6	−6.2	0.4	−5.4	0.5
だ	−2.2	0.5	−1.1	0.4	−2.8	0.4	−1.4	0.4
で	−6.1	0.6	−4.7	0.4	−5.6	0.5	−4.1	0.5
ど	−5.8	0.6	−3.4	0.5	−8.4	0.5	−4.8	0.4
ば	−0.5	0.6	−1.8	0.5	−2.6	0.5	1.0	0.6
び	−5.6	0.6	−6.3	0.7	−9.8	0.7	−6.7	0.7
ぶ	−8.1	0.7	−7.8	0.5	−10.5	0.6	−7.3	0.7
べ	−7.0	0.6	−5.1	0.6	−7.3	0.6	−6.1	0.7
ぼ	−1.5	0.5	0.1	0.7	−7.1	0.5	−5.4	0.4
ぱ	0.1	0.5	−2.8	0.5	−0.9	0.7	1.6	0.4
ぴ	−6.7	0.9	−6.4	0.7	−8.5	0.4	−7.1	0.7
ぷ	−7.6	0.7	−5.3	0.4	−12.0	0.7	−6.8	0.5
ぺ	−7.5	0.5	−4.9	0.7	−5.5	0.5	−5.5	0.4
ぽ	−1.8	0.8	−0.8	0.4	−1.7	0.4	−2.1	0.7
きゃ	−2.5	0.6	−1.4	0.5	−0.8	0.4	−1.9	0.4
きゅ	−4.6	0.5	−8.2	0.6	−8.7	0.7	−6.9	0.7
きょ	−4.8	0.4	−1.4	0.5	−4.1	0.4	−3.8	0.6
しゃ	−0.8	0.6	−1.6	0.3	−2.3	0.3	−1.4	0.4
しゅ	−7.5	0.6	−6.5	0.6	−9.6	0.6	−8.9	0.6
しょ	−6.2	0.5	−4.5	0.6	−3.5	0.6	−3.1	0.5
ちゃ	−1.3	0.6	−0.7	0.6	−0.7	0.5	−0.6	0.6
ちゅ	−7.3	0.4	−6.4	0.8	−9.9	0.6	−8.4	0.5
ちょ	−5.4	0.5	−3.5	0.6	−3.4	0.3	−2.3	0.5
にゃ	−3.8	0.6	−3.2	0.5	−5.6	0.5	−1.4	0.3
にゅ	−6.3	0.8	−5.9	0.6	−7.5	0.6	−8.9	0.6
にょ	−4.8	0.5	−5.8	0.7	−3.5	0.5	−2.6	0.6
ひゃ	−0.8	0.7	−2.0	0.4	−2.1	0.4	−0.4	0.7
ひゅ	−6.1	0.7	−6.3	0.7	−11.1	0.5	−7.1	0.6
ひょ	−6.1	0.5	−3.4	0.6	−1.3	0.4	−2.8	0.7
みゃ	−3.0	0.4	−2.3	0.5	−2.2	0.3	−2.0	0.5
みゅ	−5.3	0.6	−6.5	0.5	−8.3	0.6	−7.9	0.8
みょ	−7.0	0.5	−4.5	0.6	−3.5	0.6	−5.1	0.4
りゃ	−2.5	0.4	−1.1	0.7	−7.3	0.6	−2.4	0.4
りゅ	−7.9	0.5	−4.5	0.8	−8.4	0.6	−6.1	0.7
りょ	−4.6	0.7	−3.8	0.7	−3.6	0.5	−3.6	0.7
ぎゃ	−1.7	0.4	−2.0	0.5	−5.1	0.5	−3.1	0.6
ぎゅ	−8.1	0.8	−5.9	0.7	−9.5	0.6	−7.6	0.6
ぎょ	−4.2	0.5	−3.7	0.5	−8.4	0.5	−2.9	0.5
じゃ	−1.8	0.3	−1.7	0.4	−1.5	0.4	−3.0	0.4
じゅ	−7.6	0.5	−6.1	0.5	−10.0	0.5	−7.9	0.6
じょ	−5.9	0.6	−3.6	0.6	−2.6	0.5	−4.2	0.6
びゃ	−2.2	0.5	−1.6	0.4	−5.0	0.5	−2.4	0.5
びゅ	−7.1	0.5	−5.6	0.6	−7.8	0.5	−6.5	0.5
びょ	−4.7	0.4	−4.0	0.6	−5.8	0.6	−3.7	0.8
ぴゃ	−0.6	0.5	−2.5	0.4	−1.8	0.6	−1.8	0.5
ぴゅ	−7.8	0.9	−5.5	0.5	−7.6	0.7	−5.5	0.6
ぴょ	−4.9	0.5	−2.7	0.6	−1.8	0.4	−3.4	0.5

図-1 母
/a/に
まれる
ロット
節間の

れること
等しくな
るために
であるこ
音節聴取
指標では
今後，
表により
れらの
たい。(

表-1
のを図-
が/a/で
(12 音節
節) に
ベルを
音節に
は，2 な
が等しく
騒音レ
原因と
激の感
用は適
を表す

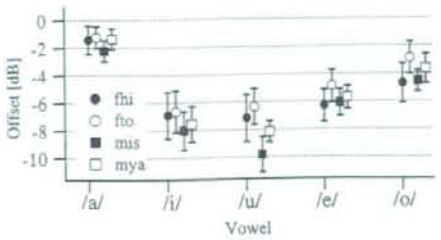

図–1　母音別の平均ラウドネス補正値
/a/には，母音/a/と，後続母音が/a/である単音節が含まれる。/i/，/u/，/e/，/o/についても同様である。プロットは表–1 に示した校正値の平均値，エラーバーは音節間の標準偏差を示す。

れることを示している。表–1 より，等価騒音レベルが等しくなるように調整した場合には，ラウドネスを揃えるために音節によっては最大 12 dB 以上の補正が必要であることを示している。このことは，少なくとも単音節聴取時の聴感レベルは等価騒音レベルという物理指標では正確に表すことができないことを示している。

今後，FW03 語表を聴取実験に用いる場合には，本表により呈示レベルの補正を行うことが望ましい。これらの校正値の電子データは著者までご請求いただきたい。（請求先：FW03@nagatani.ne.jp）

4. 考　　察

表–1 の結果を各話者について母音別にまとめたものを図–1 に示す。図中/a/は，母音/a/及び後続母音が/a/である単音節（全 26 音節）の平均値を示す。/i/（12 音節），/u/（24 音節），/e/（13 音節），/o/（25 音節）についても同様である。図–1 より，語音の呈示レベルを等価騒音レベルで揃えた場合，母音が/a/である音節に比して，母音が/i/，/u/，/e/，/o/である音節は，2 ないし 8 dB ほど小さく補正しないとラウドネスが等しくならないことが分かる（すなわち，同一の等価騒音レベルではラウドネスは大きく知覚される）。この原因として，単音節のような短時間かつ非定常な音刺激の感覚量を表すのに，A 特性や等価騒音レベルの適用は適切ではない可能性がある。単音節のラウドネスを表す物理指標の適切性については，今後詳細な検討が必要である。

謝　　辞

本研究は，奈良県立医科大学寄附講座住居医学研究奨励金の助成を得て行われた。また，本研究を進めるにあたり，同志社大学大学院工学研究科インテリジェント情報工学科知的機構研究室の柳田益造教授の多大なる協力を得た。この場を借りて，深く謝意を表する。

本研究は，国立身体障害者リハビリテーションセンター研究所の森浩一先生の貴重なご助言が発端となった。ここに厚く謝意を表する。

文　　献

[1] 天野成昭，近藤公久，坂本修一，鈴木陽一，“親密度別単語了解度試験用音声データセット（FW03），” NII 音声資源コンソーシアム (2006).
[2] 坂本修一，鈴木陽一，天野成昭，小澤賢司，近藤公久，曽根敏夫，“親密度と音韻バランスを考慮した単語了解度試験用リストの構築，” 音響学会誌，54，842–849 (1998).
[3] 坂本修一，吉川忠祐，鈴木陽一，天野成昭，近藤公久，“語音聴取域値に基づいた FW03 単語音声の聴感レベル校正，” 音講論集，pp. 307–308 (2005.3).
[4] 長谷芳樹，阪口剛史，細井裕司，“FW03 単音節音声のラウドネス校正，” 音講論集，pp. 609–610 (2008.3).

長谷　芳樹

2006 年同志社大学大学院工学研究科電気工学専攻博士課程（後期課程）修了。奈良県立医科大学特別研究員を経て，2008 年神戸市立工業高等専門学校電子工学科講師。博士（工学）。

橘　　亮輔

2006 年同志社大学大学院工学研究科知識工学専攻博士課程（前期課程）修了。現在，同志社大学大学院生命医科学研究科生命医科学専攻博士課程（後期課程）在学中。修士（工学）。

阪口　剛史

2002 年同志社大学大学院工学研究科電気工学専攻博士課程（後期課程）修了。現在，奈良県立医科大学助教。博士（工学）。

細井　裕司

1975 年奈良県立医科大学卒。近畿大学医学部助手，講師，助教授を経て，1999 年奈良県立医科大学教授。医学博士。

軟骨導音の方向感に関する基礎的検討*

○阪口剛史，△斉藤修，細井裕司（奈良医大）

1 はじめに

外耳道閉鎖症や鼓膜大穿孔などを有する症例においては，伝音系の損失を補うために，骨導補聴器や骨固定型補聴器(BAHA®: Bone Anchored Hearing Aid)を用いた補聴が行われることがある。しかしながら，骨導補聴器の使用には，

- 振動子の圧着
- 振動子の固定

の必要があるなどの欠点が伴い，BAHA®においては，

- 台座の埋め込み手術が必要
- 台座の「ねじ込み過ぎ」に伴う，頭蓋骨貫通の危険性
- 術部からの感染の危険性

などの問題点があることが否定できない。

そこで我々は前報[1]において，振動子固定に伴う痛みがなく，手術も必要としない，新たな補聴手法である軟骨導補聴を提案し,その有用性に関する基礎的検討を報告した。

今回，軟骨導補聴器を試作し，両側外耳道閉鎖症患者がそれを装用したときの自由音場における聴力を測定した。また，左耳に気導補聴器，右耳に軟骨導補聴器を装用し，被験者が両耳聴をおこなったときの，聴取音の方向感について測定したので併せて報告する。

2 方法

2.1 対象

被験者は，11 歳男児の両側外耳道閉鎖症患者 1 名とした。本症例は，聴力が右 70 dB，左 56 dB の伝音性難聴であったことから，4 歳から骨導補聴器を使用していたが，骨導振動子の圧着で次第に耳後部が陥凹した。そのため，骨導補聴器の継続的利用に当人が難色を示したことから，左外耳道の骨性閉鎖を削り，外耳道および鼓膜形成を行う手術が行われた。その術後は，聴力に改善が認められ，補聴器が不用な期間もあったが，後の形成鼓膜の浅在化などから，現在は気導補聴器を左耳に装用している。補聴器装用は，左耳のみで右耳にはしていない。

Fig. 1 は，自由音場において測定した現在の聴力を示している。本聴力測定は，オージオメータ AA-76(RION) およびスピーカ A822(JBL)を用い，本学附属病院聴力検査室内の防音室にて行われた。ただし，気導補聴器 HB-15(RIONET)の設定は，被験者が通常使用している設定とした。

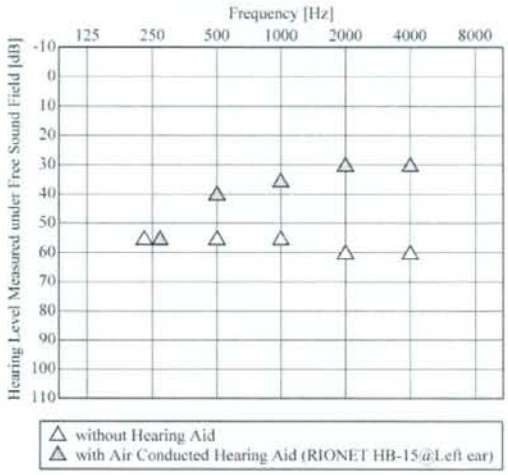

Fig. 1 Hearing level measured under free sound field.

2.2 軟骨導補聴器（試作器）の装着

試作した軟骨導補聴器を Fig. 2 に示す。本器は，箱形補聴器を改造したもので，音呈示用の軟骨導振動子と，電源，マイクロホン，増幅回路などを含む本体部から構成されている。被験者の右耳にその軟骨導補聴器を装着し，聴取音が MCP レベルとなるよう被験者自身に調整させたときの自由音場における聴力レベルを Fig. 3 に示す。ただし，このとき装用している補聴器は，右耳の軟骨導補聴器のみで，常用している左耳の気導補聴器は装

* Sound direction perception using cartilage conduction hearing-aid, by SAKAGUCHI, Takefumi, SAITO, Osamu and HOSOI, Hiroshi (Nara Medical University).

着していない。

2.3 軟骨導補聴器装用時の方向感の測定

被験者は，幼少時から右耳が高度難聴で，また，本実験を行うまで骨導・気導いずれの補聴器も左耳にのみ装用してきたことから，「これまで両耳聴はほとんどできておらず，音の方向感は体験したことがないに等しい」と実験前に語っていた。

そこで，本実験においては，被験者の「音の方向感」を以下のように簡易的に測定した。

- 被験者は，左耳に気導補聴器を，右耳には前述のように出力調整をした軟骨導補聴器を閉眼状態で装用。
- 被験者から距離 1 m 離れた話者が，被験者の前・後・左・右のいずれかに移動し「音源は前後左右のうち，どちらにありますか。」と問う。
- 被験者は，聴取音の音源の方向を口頭で回答。

3　結果および考察

試作した軟骨導補聴器を両側外耳道閉鎖症の本症例に装着させた。その結果，現在左耳に常用している気導聴力補聴器による聴力補償とほぼ同程度の補償が軟骨導補聴器単体で可能であることが分かった。

また，本症例の左耳に気導補聴器，右耳に軟骨導補聴器を装着させ，音の方向感に関する簡易な検査を行ったところ，誤答も若干見られたが，正答率 85 %と両耳聴が行われている可能性が示唆される結果が得られた。

本実験で行った軟骨導補聴器による補聴は，初めに述べた既存の骨導補聴器や BAHA®の問題点を解消し，かつ，骨導音では困難であると考えられている「音の方向感の知覚」についても優位性がある可能性が示唆される。このことは，外耳道閉鎖症などの症例，特に本症例のような両側外耳道閉鎖症の患者に対しては，有用な補聴手段となり得ることが示唆された。

Fig. 2 Cartilage conducted hearing aid (prototype).

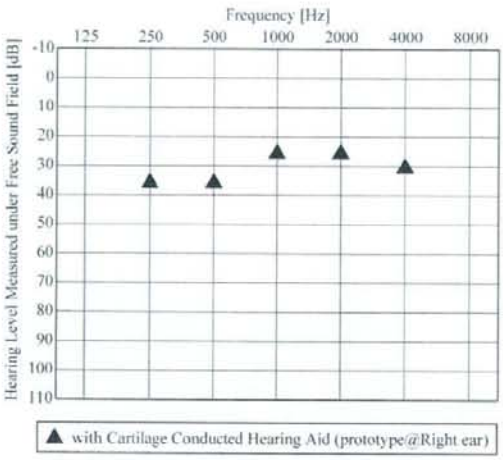

Fig. 3 Hearing level measured under free sound field.

trial	direction of the speaker	answer of the listener	
1	rear	rear	correct
2	front	front	correct
3	rear	left	wrong
4	left	right	wrong
5	right	right	correct
6	front	front	correct
7	rear	rear	correct
8	left	left	correct
9	left	left	correct
10	front	front	correct
11	right	right	correct
12	left	left	correct
13	rear	rear	correct

Fig. 4 Direction of the sound source and the listener's answer.

謝辞

本研究の一部は，文部科学省　科学研究費補助金　(18390462)の補助を受けて行われた。

参考文献

[1] 阪口，細井，音講論 (春)，555-556，2008.

45 軟骨導補聴の基礎的検討

○阪口剛史、細井裕司
奈良県立医科大学　医学部　耳鼻咽喉・頭頸部外科学講座

【はじめに】

外耳道閉鎖症や鼓膜大穿孔などを有する症例においては、伝音系のロスを補うために、骨導補聴器を用いた補聴が行われることがある。しかしながら、骨導補聴器の使用には、

・振動子の圧着
・振動子の固定

の必要があるなどの欠点が伴う。振動子の長時間の圧着は、痛みを伴うことが多く、敬遠されることが少なくない。また、振動子の固定には、ヘッドバンド様のもの、あるいは、眼鏡の蔓などが用いられることが多いが、「ずれやすい」であるとか、「美容が著しく損なわれる」などといったことから、患者サイドの評判は決してよいとは言えない。

これらの欠点を解消すべく、頭蓋骨にチタン製の台座をねじ込み、その台座を外部から加振し振動させることによって骨導音を伝達させる、骨固定型補聴器(BAHA: Bone Anchored Hearing Aid)と呼ばれるものがスウェーデンで開発された。本機は、上述の固定法、あるいは、固定時の痛みに関する問題をほぼ解消することができ、かつ、骨部に高効率に音響エネルギーを伝達することが可能であることなどから、欧米を中心に普及が進みつつあり、本邦でも導入例が徐々に増えてきているようである。しかしながら、このBAHAには、

・台座の埋め込み手術が必要
・台座の「ねじ込み過ぎ」に伴う、頭蓋骨貫通の危険性
・術部からの感染の危険性

など、従来型の骨導補聴器には存在しなかった新たな問題点があることも否定できなく、その導入には慎重な検討が必要であると考えられる。

そこで我々は、外耳道閉鎖症や鼓膜大穿孔などの症例に対して有効な補聴が期待でき、かつ、前述した骨導補聴器、あるいは、BAHA導入時の問題点を有しないと考えられる新たな補聴方法として、軟骨導補聴を提案する。　軟骨導補聴とは、耳珠などの軟骨部を介して音響エネルギーの伝達を行う方法で、振動子固定に伴う痛みはほとんどなく、手術も要しないことから、外耳道閉鎖症や鼓膜大穿孔などの症例に対して十分な補聴効果が得られるようであれば、当該症例に対する有効な補聴手段のひとつとして成立するものと期待できる。

本報では、外耳道閉鎖症患者に対して聞こえの検査を行い、その結果をもとに軟骨導補聴の補聴効果について基礎的検討を行ったので報告する。

【対象】

被験者は、両側外耳道閉鎖症患者1名とした。本症例は11歳男児で、伝音性難聴。4歳から骨導補聴器を使用していたが、耳後部は骨導振動子の圧着で陥凹した。手術で、外耳道の骨性閉鎖を削り、また、外耳道および鼓膜形成が行われた後、聴力に改善が認められ、補聴器が不用な期間もあったが、後の形成鼓膜の浅在化などから、現在は気導補聴器を使用するようになっている。

また、比較のため、耳科学的正常者1名についても検査を行った。

【聴力検査】

上述の被験者に対して、下記の聴力測定を行った。

・裸耳聴力の測定

・骨導聴力の測定

・気導補聴器装用時の聴力を想定した挿入型イヤホンを用いた聴力測定

・軟骨導聴力の測定（fig. 1に示すように、試作した軟骨導音呈示用振動子を被検耳の耳珠に固定して測定）

これら測定には、オージオメータ AA-7A (RION)、挿入型イヤホン EARTONE 3A (Cabot Safety Corporation)および軟骨導音呈示用振動子（試作品）を用いた。

なお、挿入型イヤホンは、JIS規格に準拠して事前に校正されたものを使用した。軟骨導聴力のHL表示換算には、加速度ピックアップ BK4508B (B&K)を用い測定した、軟骨導音呈示用振動子、および、オージオメータ付属の骨導振動子 BR-41 (RION)の出力時の加速度を使用した。

【結果および考察】

外耳道閉鎖症の本症例に対して行った

(a) 挿入型イヤホンによる聴力測定

(b) 骨導聴力測定

(c) 軟骨導聴力測定

の結果を fig. 2 に示す。

気導聴力は鼓膜が浅在化しているため 50 dB 程度であったが、骨導聴力は、2 kHz を除いて正常であった。軟骨導聴力は、術側である左耳については、ほぼ正常の閾値を得た。非術側である右耳については、外耳道の骨性閉鎖の影響か 30 dB 程度の聴力となっていた。

本実験で行った軟骨導による補聴は、骨導のような振動子の強い圧着を必要とすることなく、耳珠に振動子を軽く接触させることで十分な補聴効果が得られたこと、また、耳漏のある耳に対しても適応可能であることから、骨導補聴器やBAHAが適応となるような外耳道閉鎖症などの症例に対して有用な補聴手段となり得ることが示唆された。

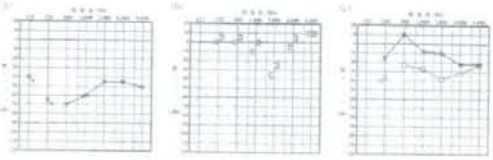

総 説

突発性難聴の診断と治療

奈良県立医科大学　耳鼻咽喉科学教室
西 村 忠 己

1．はじめに

突発性難聴は、突然片方の耳が聞こえなくなってしまう疾患で、その原因は不明である。突然おこる難聴（突発難聴）の原因には、音響暴露、頭部打撲などの外傷、中耳炎、内耳炎、鼓膜炎などの炎症性疾患や高血圧、糖尿病など様々あるが、本疾患ではそれらいずれの原因も認められない。発生率は年間ほぼ10万人に10人前後と言われているが近年増加傾向にある[1),2)]。好発年齢は30から60歳ぐらいで、発生率に性差はない[1)]。本疾患で重要なことは、できるだけ早期に治療を行った方が効果があると考えられているため、速やかに診断し治療を開始することである。突然の難聴を主訴に来院すれば突発性難聴を疑うことは容易であるが、注意すべきことは必ずしも難聴を訴えない例があることである。本疾患を見落とさず診断治療行うため、本疾患の症状、経過および診断方法について知っておく必要がある。本稿ではそれらの点に加え、鑑別を要する疾患や本疾患の治療法、予後について簡単に解説した。

2．病因

原因不明のものを突発性難聴としているため、原因は明らかでない。原因として推定されているものに、循環障害説、ウイルス説、内耳窓破裂説、アレルギー説などある[3),4)]。症例ごとに聴力障害の程度、めまいの有無、聴力経過、治療効果などが異なることから、突発性難聴のすべての症例が単一の原因により引き起こされるものとは考えにくく、さまざまな病態の疾患が集まった症候群であると考えられている。

3．症状

突然起こる一側性の難聴が特徴である。発症後数日間は聴力障害が進行する場合があるが、それ以降は悪化することは通常ない。難聴以外の症状として突然に起こった耳鳴を自覚する症例が多い。このような耳鳴を訴える例では難聴の訴えが無くても本疾患の可能性を考える。耳鳴を主訴に来院し、難聴を自覚していない症例が実際に存在しており、このような症例では、片耳聞こえているため会話に支障がないことに加え、耳鳴の症状が強いため難聴に気づいていないものと思われる。また電話で初めて音が聞こえていないことに気づき来院した症例もある。その他の蝸牛症状としては耳閉感や音が響く感じを訴える症例がある。めまいなどの前庭症状については30－50％ぐらいとあるといわれている[1)]。めまいについては一過性である。本疾患では第８脳神経以外の他の神経症状は示さない。他の神経症状を示す場合は他の疾患を考える。

4．診断基準と重症度分類

表１に厚生省特定疾患突発性難聴調査班研究の診断の手引きを示す。海外では基準があいまいで、報告ごとにことなるが、本邦では同班研究の診断基準により診断される。診断および重症度を分類するためには純音聴力検査が必要となる。聴力障害の程度は純音聴力検査の250、500、1000、2000、4000Hzの５つの周波数の閾値の平均値（５分法平均値）で評価する。初診時の聴力が悪いほど聴力の回復が少ないといわれている[4)]。その他の聴力の予後に影響を与える因子としてめまいの有無、治療開始までのかかった日数が重要であると考えられている[1),3)]。めまいの有る症例は無い

症例と比較して有意に回復が悪いと多くの文献で報告されている。治療開始までの日数については、できるだけ早期に治療を開始したほうが聴力の回復が良いとの報告が多い。しかし突発性難聴は自然治癒がある疾患のため、治療開始までの日数の影響については厳密な比較ができないことから、これを否定している文献もある[5]。現時点では治療を行っても治癒しない症例があることも事実であることから治療についてはできるだけ早期に開始したほうが良いという意見が多い。これらの突発性難聴の予後に与える影響を考慮した重症度分類が厚生省特定疾患突発性難聴調査班研究より提案されており、突発性難聴の評価に用いられている（表2）。

5．鑑別診断

突発性難聴は症候群であり、その原因は多岐にわたる。初診時にはその症状と聴力検査より診断するが、その後の経過で突発難聴の原因疾患が判明する場合がある。診断には以下に挙げる疾患の可能性について念頭に置き、注意深く診断し経過を見ていく必要がある。

表1　突発性難聴診断の手引き（厚生省特定疾患突発性難聴調査班研究、1973年）

Ⅰ．主症状

1．突然の難聴

文字どおり即時的な難聴、または朝、目が覚めて気づくような難聴。

2．高度な感音難聴

必ずしも「高度」である必要はないが、実際問題として「高度」でないと突然難聴になったことに気づかないことが多い。

3．原因が不明、または不確実

つまり、原因が明白でないこと。

Ⅱ．副症状

1．耳鳴り

難聴の発生と前後して耳鳴りを生ずることがある。

2．めまい、および吐き気、嘔吐

難聴の発生と前後してめまいや、吐き気、嘔吐を伴うことがあるが、めまい発作を繰り返すことはない。

3．一側性の場合が多いが、両側性に同時罹患する例もある。

4．第Ⅷ脳神経以外に顕著な神経症状を伴うことはない。

診断基準

確実例：Ⅰ．主症状、
　　Ⅱ．副症状の全事項をみたすもの．

疑い例：Ⅰ．主症状の1．2．の事項をみたすもの

参考

1．Recruitment現象の有無は一定せず。

2．聴力の改善・悪化の繰り返しはない。

表2　突発性難聴の重症度分類（厚生省特定疾患急性高度難聴調査班、1998年）

重症度	初診時純音聴力
Grade 1	40dB未満
Grade 2	40dB以上　60dB未満
Grade 3	60dB以上　90dB未満
Grade 4	90dB以上

注1　聴力は250、500、1000、2000、4000 Hzの5周波数の閾値の平均とする。

注2　この分類は発症後2週間までの症例に適応する。

注3　初診時めまいのあるものではaを、ないものではbを、2週間過ぎたものでは'を付けて区分する。
（例：Grade 3a、Grade 4b'）

(1)聴神経腫瘍

聴神経腫瘍の10－20％は突発難聴として発症する。これらの症例ではステロイドの点滴により、聴力が著明に回復する例も多い。しかしいったん回復した聴力は再度悪化をきたす。通常突発性難聴が再発することはなく、突発難聴を繰り返す症例ではMRI検査は必須である。聴力像の特徴として特定の周波数の閾値のみ高いnotch型やある周波数より高い周波数の音が聴取できないsharp cut型の聴力像を呈している場合要注意である。突発難聴の患者全体の中で聴神経腫瘍の割合は１％から数％といわれており、その可能性について説明しておいた方が良い。

(2)メニエール病

めまいを伴う突発性難聴の場合鑑別が必要である。突発性難聴は通常、再発しないが、メニエール病のめまい、難聴は反復するため、鑑別となる。メニエール病の診断にはその診断基準では、めまい症状、蝸牛症状の反復が必須となってくる。そのためメニエール病の初発の発作では突発性難聴との鑑別が困難である。鑑別点としてはメニエール病では低音障害型の感音難聴が多いことがあげられる

(3)外リンパ瘻

急激な圧変化の結果、内耳窓に破裂をきたし、外リンパが漏れ出すことで難聴やめまいをきたす疾患である。難聴やめまい発症時の状態についてよく問診し、力みや鼻かみなど原因となることがなかったか聞き出す必要がある。水の流れるような耳鳴りや発症時にポップ音を聞いていることがある。外耳道の加圧、減圧によるめまい、眼振、変動する聴力を示す場合要注意である。外リンパ瘻を疑った場合、ベット上安静の上ステロイドの点滴などを行い経過を見ることで回復する場合が多い。それにもかかわらず聴力の悪化が進む場合は手術を考慮する。診断の確定には試験的鼓室開放術が必要である。

(4)機能性難聴

器質的な異常がないにもかかわらず聴力検査で難聴を示す症例で、心因性難聴や詐聴がある。検診などで見つかる機能性難聴では、耳症状がない場合が多いが、病院に受診する症例では、難聴、耳閉感、耳痛などを訴える場合が多い。聴力検査で片耳の難聴を示す場合突発性難聴との鑑別は難しく、突発性難聴として治療されている場合もある。診断には聴性脳幹反応などの客観的な聴力検査が必要となるがその場で実施することは難しいことが多い。機能性難聴を疑う所見として、突発性難聴で高頻度に訴える耳鳴症状を訴える症例が少ないこと、症状に変動がある（聴こえている日と聴こえない日がある）ことなどが挙げられる。機能性難聴の症例では純音聴力検査の結果に比して言葉の聞き取りが良い例が多く、語音聴力検査を行うと純音聴力検査の結果との乖離を認める場合が多い。

(5)急性低音障害型感音難聴

聴力検査で低音域のみに起こる突発難聴でめまいは伴わない。突発性難聴と同じく原因は不明であるが、ストレスに関係している症例が多く近年増加傾向である。治療によく反応し回復するが、再発する症例も多く必ずしも予後良好な疾患ともいえない。突発難聴で低音３周波数の聴力閾値の合計が70dB以上で高音3周波数の聴力閾値の合計が60dB以下のめまいを伴わない感音難聴の場合診断される[6]。治療はステロイドやイソソルビドが用いられることが多い。

(6)ムンプス難聴

ムンプスで難聴を起こす可能性については良く知られているがその頻度２万人に１人程度である。しかしムンプスの中には耳下腺の腫脹のない例があり、IgM抗体の測定で突発性難聴と考えられた症例の中にムンプス難聴の症例が含まれていることが判明した。

(7)音響外傷

強大音の暴露を受けた後に起こる感音難聴である。突発性難聴との鑑別には音響暴露などの問診を取ることが重要である。治療は突発性難聴とほぼ同じであるが、突発性難聴と比較して回復しにくいと言われている。